

On Characterizing Cuboctahedral Fully Augmented Links

Emerson Worrell

July 22, 2022

Abstract

We give a combinatorial description for all cuboctahedral FALs that respect the preferred horoball packing, analogous to Purcell's description of octahedral FALs [5]. Additionally, we utilize the work of Adams [1] and Morgan, Ransom, Spyropoulos, and Ziegler [4] to show how this family of FALs can be belt-sum decomposed, and also find common geodesics in a subset of this family.

1 Understanding Fully Augmented Links

1.1 What is a Fully Augmented Link?

We begin by defining the class of links that we will be working with.

Definition 1.1 (Twist Region). For any link diagram L , a twist region is formed whenever exactly two strands cross in a projection of the link. For every n twists in a given twist region, exactly $n - 1$ bigons are formed.

Definition 1.2 (Fully Augmented Link). Take any link diagram L . For every twist region, place an unknotted component (known as a crossing circle) around the entire twist region and reduce the number of twists modulo 2. Thus if there are an even number of bigons, there will be only 1 twist inside the crossing circle, and if there are an odd number of bigons, the strands non-intersecting. The result is a fully augmented link (hereafter referred to as an FAL). Figure 1 provides examples of twist regions and the process of augmenting a link.

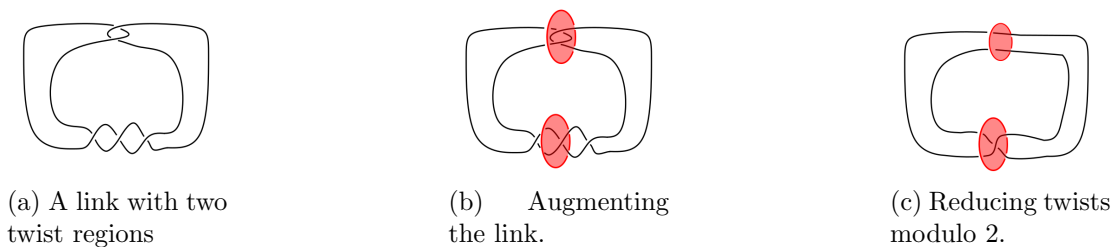


Figure 1: Fully augmenting a link.

FALs possess certain nice properties that make them worthy of study. Firstly, reducing the number of twists modulo 2 results in a complement that is homeomorphic to the original [5]. Also, the presence of half-twists does not affect the volume of the FAL. This means that for any FAL, there are up to 2^n half-twist partners (perhaps less due to symmetries) whose complements are all homeomorphic, and can be considered to be members of the same equivalency class. We say an FAL is “flat” if it contains no half-twists. Additionally, the complements of certain FALs decompose nicely in regular ideal polyhedra, which we will discuss presently.

1.2 Cell Decomposition, Circle Packings, and The Upper Half-Plane Model

Definition 1.3 (Hyperbolic FAL). An FAL F is hyperbolic if a metric of constant curvature -1 can be placed on the manifold $S^3 - F$.

Theorem 1.4 (Purcell). Let F be a hyperbolic FAL. There is a decomposition of S^3/F into two identical totally geodesic polyhedra that possess the following properties:

- Faces of the polyhedra can be checkerboard colored, with shaded faces all triangles each corresponding to one half of a crossing circle, and white faces corresponding to the link components lying in the projection plane.
- Ideal vertices are all 4-valent
- The dihedral angle at each edge is $\frac{\pi}{2}$.

Purcell’s proof for this theorem is primarily procedural, so we shall explain in briefer detail the process of cell decomposition that is used to obtain these polyhedra.

In the standad cell-decomposition, planar components and crossing circles form the 2-cells, while the intersections of these form the 1-cells. When we decompose, we first cut across the plane of projection (hence why we have two identical polyhedra, denoted P_+ , P_-) as seen in the leftmost image of Figure 2. Then, we slice along the crossing circles, splitting them into two faces. We then compress the intersection of the two halves of the crossing circles and the planar components to single points, then stretch the resulting Figure into a circle packing in the plane.

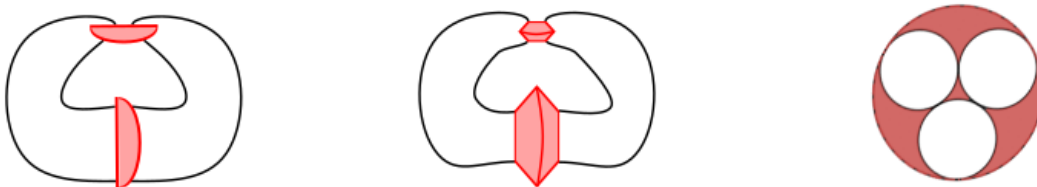


Figure 2: The cell-decomposition process.

1.3 Nerves, Crushtaceans, and Their Paintings

As mentioned, the decomposition process results in a circle packing that determines one of the two identical ideal polyhedra. We can use this circle packing to define the nerve and the crushtacean, which are tools that allow us to examine the link as a planar graph.

Definition 1.5 (Nerve). Begin with a circle packing C corresponding to some FAL F . The center of each circle in the circle packing corresponds to a vertex in the graph, while points of tangency between two circles correspond to edges. This process forms the nerve of an FAL, denoted F_N .

We can also choose to color the nerve in the manner described in the following:

Definition 1.6 (Painted Nerve). If the point of tangency in a circle packing is shared by two halves of the same crossing circle, then the corresponding edge in the graph will be painted. If not, then it will be unpainted (black). This process forms the painted nerve of an FAL.

We also cite a result from Purcell regarding the nerve:

Theorem 1.7 (Purcell). Let F be a hyperbolic FAL. Then the nerve F_N is a triangulation of S^2 , and satisfies the following properties:

- Each edge of the nerve has distinct endpoints.
- No two vertices are joined by more than one edge.
- If γ is a triangulation of S^2 satisfying the above properties, then any painting of γ such that each triangle has exactly one painted edge is considered to be “well-painted”, and the well-painted γ corresponds to an FAL.

Definition 1.8 (Crushtacean). The crushtacean is the dual graph to the nerve, denoted F_C . It is formed by creating a vertex for every triangle in $S^2 - F_N$, and each edge corresponds to when two triangles border each other (share an edge). If the shared edge between two triangles in F_N is painted, then the corresponding edge in F_C is also painted, and unpainted otherwise.

The crushtacean provides an easy way to move from a graph to its corresponding FAL, as each painted edge corresponds to a crossing circle, and each vertex of these painted edges receive exactly two unpainted edges, which correspond to planar components. Figure 3 shows the formation of a painted nerve from a circle packing and its corresponding crushtacean.

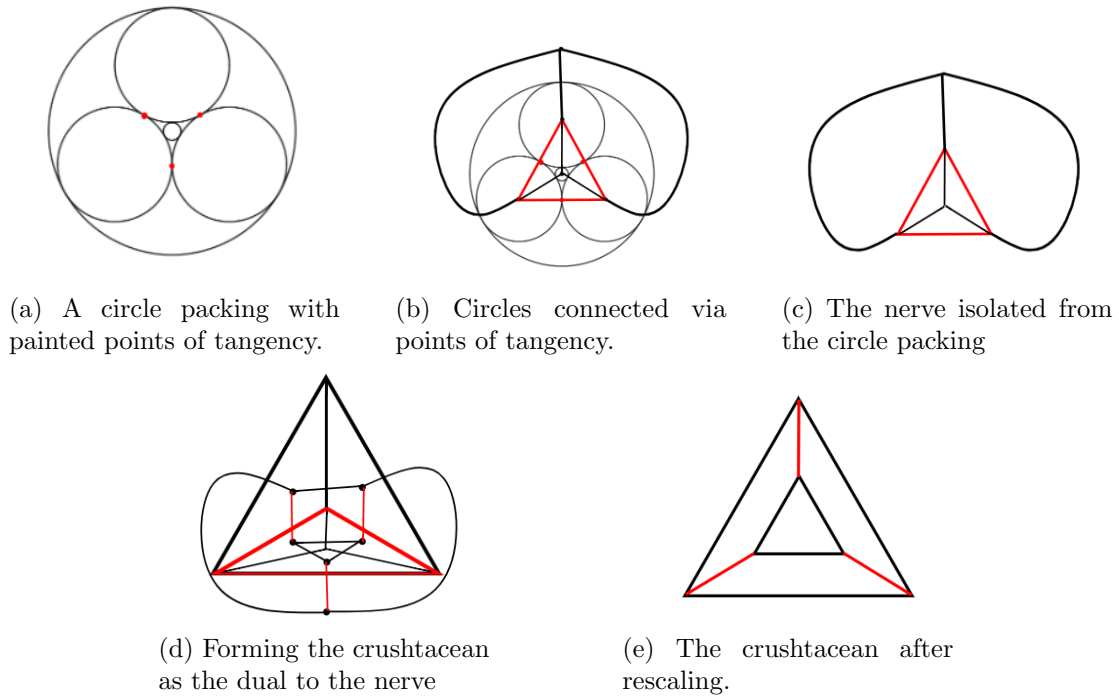


Figure 3: Moving from a circle packing to a crushtacean

2 Characterizing the Nerves of the 1st Family of Cuboctahedral FALs

Purcell’s paper provides a complete combinatorial description, using unpainted nerves, for all octahedral FALs whose decomposition respects the preferred horoball packing. In this paper, we will provide a similar description for the family of cuboctahedral FALs which decompose into cuboctahedra in the same manner as in Purcell’s work. We will henceforth refer to this family as the 1st family of cuboctahedral FALs.

2.1 The Basic Building Block, P_4

Purcell began her proof using the simplest octahedral FAL, the Borromean Rings, which is formed from two regular ideal octahedra. We follow a similar route, using the simplest cuboctahedral FAL, formed by only two regular ideal cuboctahedra: the chain of eight links, hereafter referred to as P_4 , using the notation from [Meyer/Millichap/Trapp] [3]. Note that from here onwards, whenever we say cuboctahedron we are referring to a regular ideal cuboctahedron. Additionally, while we only say P_4 , we are including its equivalence class of half-twist partners. We preface the proof of this result by first finding the circle packing of P_4 . Next, we may send one of the points of tangency to infinity using a Möbius transformation, all of which is shown in Figure 4.

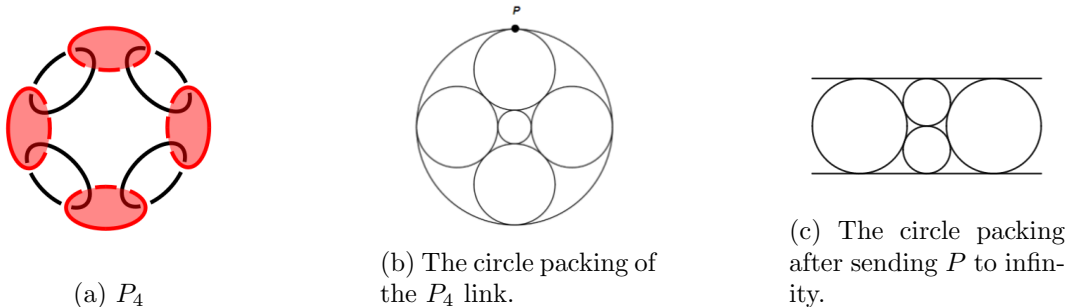


Figure 4: P_4 and its circle packing.

We also define a specific form of subdivision that we will utilize:

Definition 2.1 (Central Triangular Subdivision). Take any graph that is a triangulation of S^2 . To perform *central triangular subdivision* on this graph, take any triangle, and insert another triangle inside it so the sides of the new triangle face the vertices of the exterior triangle. Then, connect the two vertices of each side of the interior triangle to the corresponding vertex in the exterior triangle.

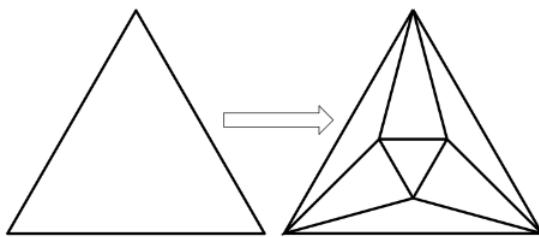


Figure 5: Central triangle subdividing a triangle

We now define a family of cuboctahedral FALs that respect the preferred horoball packing as defined by Purcell.

Definition 2.2 (The 1st Family). The 1st family of Cuboctahedral FALs contains all cuboctahedral FALs whose decompositions respect the preferred horoball packing, i.e the manner of decomposition described in Section 1. Equivalently, this is all cuboctahedral FALs whose upper and lower halves P_+ and P_- contain an integer number of cuboctahedra, and no cuboctahedra are split between the two halves.

We include one last definition for ease of communication:

Definition 2.3 (Simple Cuboctahedral Nerve). We refer to the unpainted nerve of P_4 shown in Figure 6 as the simple cuboctahedral nerve.

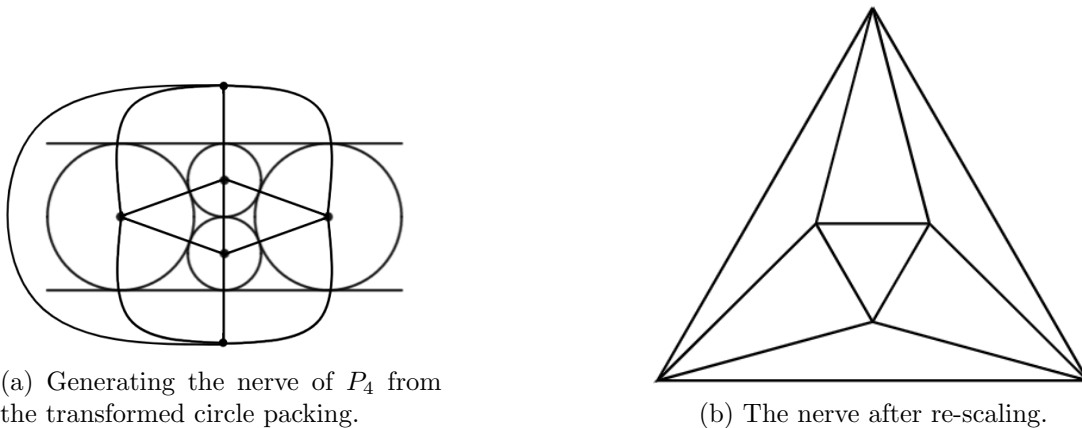


Figure 6: Finding the nerve of P_4 .

2.2 The Primary Result of This Section

Lemma 2.4. If the two identical polyhedra formed by the decomposition of an FAL are formed by gluing multiple regular ideal cuboctahedra together, then the cuboctahedra must be attached to each other along shaded faces.

Proof. Let P be formed by gluing two regular ideal cuboctahedra together. They then must share at least one vertex, which we map to infinity under a Möbius transformation. Suppose by way of contradiction that they are glued by attaching unshaded faces to each other. Then we will have two copies of Figure 4c glued along the one of the horizontal lines. But this means that the shaded faces at the ends of the Figure will become quadrilaterals, having 3 ideal points in the plane and one at infinity. But this violates the checkerboard criterion in Theorem 1.4, so we must have to glue them along shaded faces.

Each time we glue an additional cuboctahedron with a point at infinity, we must continue to glue along shaded faces or else we violate Theorem 1.4. Additionally, if we glue a cuboctahedron to the structure that has no points at infinity, it must be along once of the interstices in the circle packing. This is essentially attaching a cuboctahedron “underneath” the polyhedron it is being glued together with. \square

Lemma 2.5. Gluing a cuboctahedron to a polyhedron along a shaded face is represented in the circle packing by filling an interstice with three mutually tangent circles, each of which are tangent to two of the circles forming the interstice.

Proof. We need to add circles into the circle packing in such a way that the new points of tangency form a cuboctahedron using the dual circles connecting them. We know from Lemma 2.4 that we must glue shaded faces together. A cuboctahedron has exactly 6 quadrilateral faces and 8 triangular faces; each vertex of a cuboctahedron joins two quadrilateral and two triangular faces together, and faces of the same shape never share

an edge.

Consider some interstice formed by three circles. If we fill this interstice with three mutually tangent circles that each touch two of the bounding circles, we get Figure 8. The addition of these three circles inside the interstice forms 7 shaded triangular faces and 6 unshaded quadrilateral faces, 3 of which lie outside the interstice. The final unshaded face is the entire interstice itself, to which the additional cuboctahedron was glued. So this manner of adding circles corresponds to gluing one additional cuboctahedron. \square

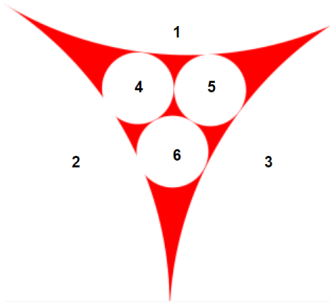


Figure 7: Adding a cuboctahedron in the circle packing. The 6 unshaded quadrilateral faces are numbered, and the 7 visible triangles are the shaded interstices.

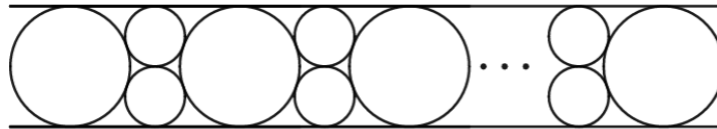


Figure 8: N Cuboctahedra glued together linearly.

Theorem 2.6. Let F be a cuboctahedral FAL with nerve F_N . Then F is a member of the 1st family if and only if F_N is formed through repeated central triangular subdivision on the simple cuboctahedral nerve.

Proof. Suppose F is a member of the first family. Then each of the two identical polyhedra that F decomposes into must be formed by exactly n cuboctahedra, for some $n \in \mathbb{N}$. We can use a Möbius transformation to send one vertex of these polyhedra to infinity. Since the polyhedra are identical whatever holds for one holds for both, so we can consider just P as one polyhedra representing both P_+ and P_- . Since P is formed by gluing cuboctahedra together, the vertex at infinity will be the vertex of at least one cuboctahedron.

If P is formed by only 1 cuboctahedron, then after sending a vertex to infinity it must be of the form shown in Figure 4c. The nerve of this circle packing is shown in

Figure 6. Suppose P is made from n cuboctahedra. When the second cuboctahedron was attached, it must have been attached along a shaded face in the manner described by Lemma 2.5. Suppose without loss of generality that we glued the second cuboctahedron to the face on the right with a point at infinity. Then we get a circle packing as shown in Figure 9a. Figures 9b and 9c show the nerve of this circle packing. This is the simple cuboctahedral nerve with central triangular subdivision performed once. For every additional cuboctahedron we attach, we add three circles into an interstice, which will correspond to central triangular subdivision of the corresponding triangle in the nerve. So the forward direction is proven.

Now suppose F is some FAL with nerve F_N , where F_N is the result of some number of central triangular subdivisions. For each of these subdivisions, we add exactly 3 vertices and 9 edges inside one of the triangles in the nerve. This corresponds to adding 3 mutually tangent circles into an interstice, each of which touches 2 of the exterior triangles forming the interstice, which by Lemma 2.5 is equivalent to gluing an additional cuboctahedron. So the reverse direction is proven. \square

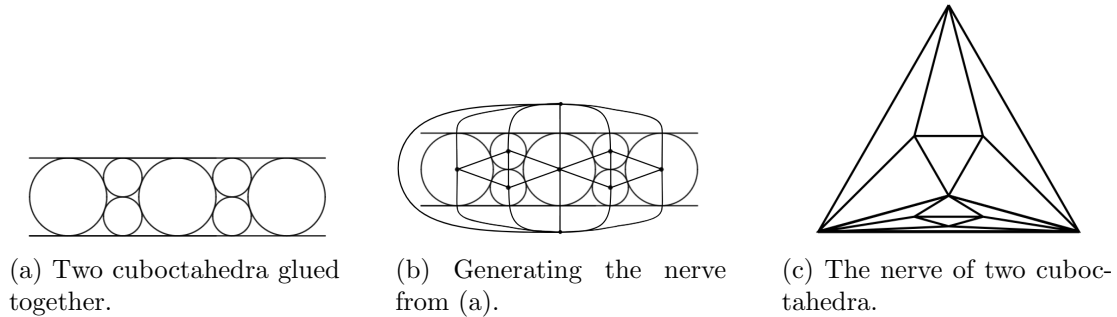


Figure 9: The nerve of 2 cuboctahedra

To see what an arbitrary 1st family member's nerve may look like, see Figure 10.

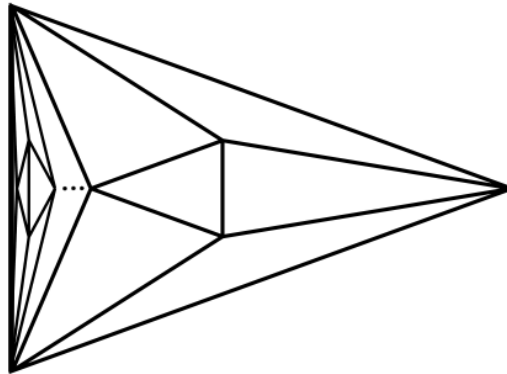


Figure 10: The nerve of n cuboctahedra.

We end this section with a corollary to the previous theorem that relates the number of crossing circles in a 1st family member to the number of cuboctahedra in its complement.

Corollary 2.6.1. The number of cuboctahedra in the complement of a 1st family member is $\frac{2}{3}(c - 1)$, where c is the number of crossing circles.

Proof. If F is a member of the 1st family, then its nerve F_N is a triangulation of S^2 by Theorem 1.7. Since the nerve must be well-painted, each triangle has exactly one painted edge. Since each painted edge borders two triangles, and each painted edge corresponds to 1 crossing circle, the number of crossing circles c is the number of triangles T in the nerve divided by two, or $c = \frac{T}{2}$.

Additionally, since F_N is a triangulation of S^2 , $3T = 2E$, where E is the number of edges in the nerve. Finally, we have $E = 9n + 3$, where n is the number of cuboctahedra. This comes from there being 12 edges in the simple cuboctahedral nerve, and with each subdivision 9 edges are added. Putting this all together with some algebra yields $n = \frac{c-1}{3}$. But this corresponds only to P_+ . For every cuboctahedra in P_+ , there is one in P_- , and the nerve only corresponds to one of the halves of the complement of F . So we multiply by a factor of 2, getting the desired expression. \square

3 Characterizing the 1st Family in Terms of Belted Sums

Now that we have a complete combinatorial classification of the 1st family of cuboctahedral FALs, we may change directions and use this result to describe the first family in a different manner. In this section, we will define the belt-sum operation for FALs, what it means to be belt-sum prime, and how all 1st family cuboctahedral FALs are formed as belted-sums of two specific cuboctahedral FALs.

3.1 Necessary Background

Belt-summing is an operation defined by Adams where two FALs can be joined in a manner that preserves volume. This occurs by slicing along thrice-punctured spheres in the complements of the links and the gluing together along the cut. The result is one FAL whose volume is the sum of the previous two.

There are a number of definitions and theorems that must be referenced before we begin explaining our results. The work in this section is primarily an extension of the work done by Morgan, Ransom, Spyropoulos and Ziegler from the CSUSB REU in 2017 [4], and as such much of this background information is their original research, which we shall cite but not explain in detail.

Definition 3.1 (Non-Trivial 3-Cycle). A non-trivial 3-cycle in a nerve is any 3-cycle that does not bound a face when considering the nerve as a triangulation of S^2 .

Definition 3.2 (Buckle). A buckle is defined as a non-trivial, once-painted 3-cycle.

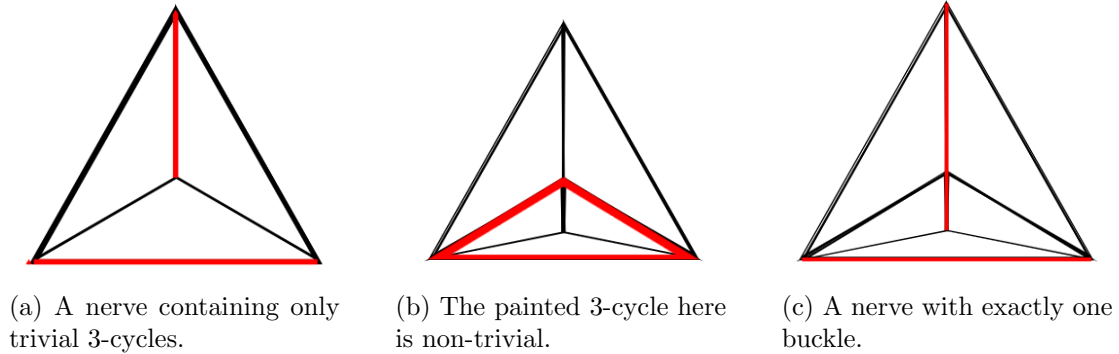


Figure 11: Buckles and 3-cycles.

Lemma 3.3 (Morgan et. al.). Every 3-cycle in a well-painted nerve F_N is either once-painted or thrice-painted.

Theorem 3.4 (Morgan et. al.). An FAL is the belted sum of two others if and only if its painted nerve contains a buckle.

Corollary 3.4.1 (Morgan et. al.). F is belt-sum prime if and only if its nerve contains no buckles.

Theorem 3.5 (Morgan et. al.). The following statements are all true:

- Each FAL has a belt-sum decomposition into belt-sum prime FALs.
- This decomposition is commutative.
- This decomposition is unique.

The above theorems are not trivial, but for our purposes we may take them for granted and use them as is relevant to our topic. The last theorem in particular is quite strong, and will be utilized heavily in this section.

3.2 There Are Only Two Well-Paintings of the Simple Cuboctahedral Nerve

Our goal now is to find all belt-sum prime cuboctahedral FALs, so to begin, we may start with the simplest. The unpainted nerve of P_4 is the simplest cuboctahedral nerve, and as shown in the previous section, every cuboctahedral FAL is formed by subdividing this nerve. We may start by finding every well-painting of this nerve:

Theorem 3.6. The two painted nerves found in Figure 12 below are the only two well-paintings of the simple cuboctahedral nerve.

Proof. We must find every way to paint this graph so that each triangle has exactly one painted edge. There are exactly 8 triangles including the exterior triangle, so we must paint exactly 4 edges. Since the exterior triangle must have a painted edge, without loss of generality we may paint the bottom edge of this triangle (this comes from the rotational symmetry of the nerve). Now we have two triangles with painted edges, leaving 6 unpainted. From here, we also must paint the interior triangle. Up to symmetry there are only two ways to do this: painting the upper edge or painting one of the lower edges. From here, each of these nerves can only be painted in one way in order to well-paint the entire nerve. So there are only two well-paintings of the simple cuboctahedral nerve. \square

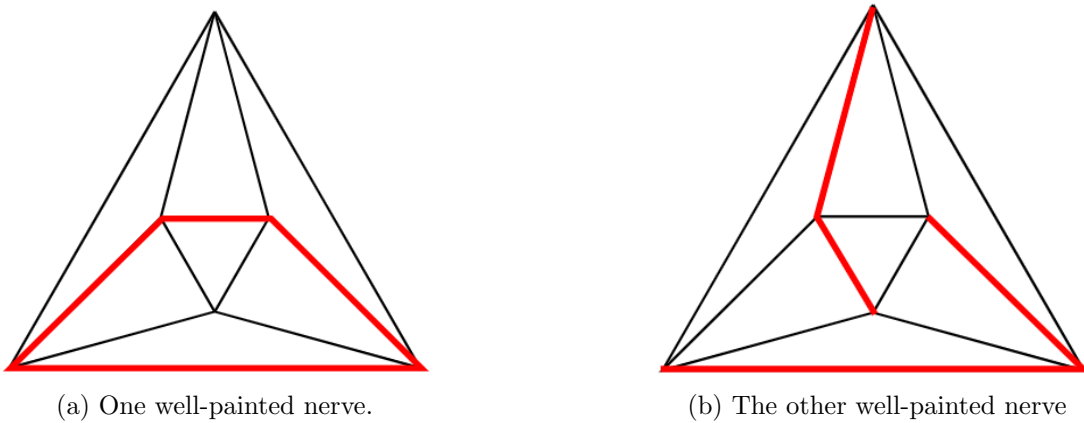


Figure 12: The two well-painted simple cuboctahedral nerves.

Corollary 3.6.1. The two painted nerves in Figure 12 are belt-sum prime.

Proof. This comes as a direct consequence of the previous theorem. These nerves are well-painted by construction, and they contain no non-trivial 3-cycles, therefore they can't contain a buckle. So by Corollary 3.4.1, these nerves are belt-sum primes. \square

It is worth examining what flat FALs these two nerves correspond to. These are shown in Figure 13. Naturally, one of these is P_4 . The other is a link with only 3 planar components; we will refer to this link C_2 , as it is the second cuboctahedral FAL in the 1st family. We are unsure if this link has another given name or if it has been studied in the past.



Figure 13: The two FALs corresponding to the nerves in Figure 12.

3.3 Any Central Triangular Subdivision of The Simple Cuboctahedral Nerve Must Form a Buckle

Next, we may consider central triangular subdivisions of this nerve, as all other members of the 1st family are simply well-paintings of some arbitrary number of central triangular subdivisions of this nerve. Those that contain no buckles will be the remaining belt-sum prime FALs that we are looking for. But as it happens, there are none of this form, as detailed in the theorem below:

Theorem 3.7. Any central triangular subdivision of the simple cuboctahedral nerve must form a buckle.

Proof. Let F_N be the painted nerve corresponding to some 1st family member that is not P_4 or C_2 . Then by Theorem 2.6, F_N must have been subdivided at least once. Consider the “innermost” subdivision(s) (see Figure 14). We know that there must be an innermost subdivision, because if not, then there would be infinitely many subdivisions corresponding to infinitely many cuboctahedra, which is impossible for an FAL with finitely many components.

Now consider the exterior triangle of this subgraph. By Lemma 3.3, this 3-cycle is either once painted or thrice-painted. If it is once-painted, then it is by definition a buckle.

If it is thrice-painted, then we now must attempt to paint the interior edges so that the subgraph is well-painted. The three outermost triangles of this subgraph already have one painted edge, so there are 4 remaining triangles to paint, meaning we must carefully select two edges to paint. Up to symmetry, there is only one way to paint an edge of the interior triangle, so without loss of generality, we may paint the top edge of this triangle. But now we face a predicament! There are two unpainted triangles that do not share an edge (see Figure 15). Therefore, we cannot well-paint this graph. As a result, it means that if F_N is a nerve that has been subdivided at least once, it must contain a buckle, since every non-trivial 3-cycle will be once-painted. \square

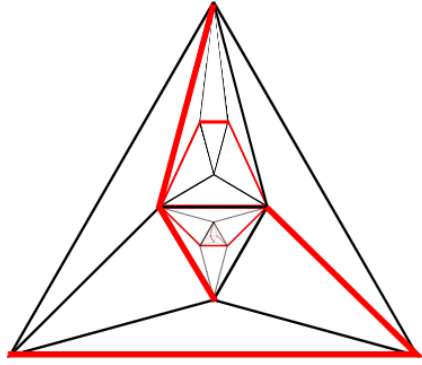


Figure 14: The subdivision in the very center (look closely!) and in the top center are the two innermost subdivisions, as they are simple cuboctahedral nerves that have not been subdivided further.

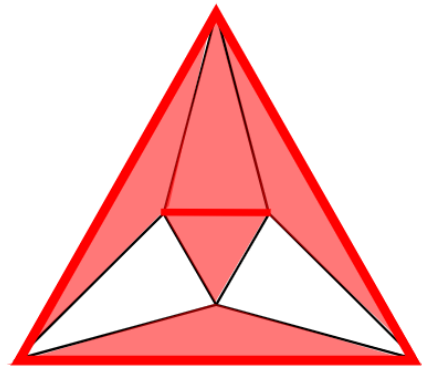


Figure 15: We are left with two triangles that have no painted edges (the exterior triangle has a painted edge, but was not filled in for visual clarity).

3.4 There Are Only Two Belt-Sum Prime 1st Family Members

We now reach the main result of this section:

Theorem 3.8. The only two belt-sum prime 1st family members are P_4 and C_2 , and their half-twist partners.

Proof. Let F be a cuboctahedral FAL, and let F_N be its painted nerve. Then either F_N has been subdivided or it hasn't.

Case 1: If F_N hasn't been subdivided, then by Theorem 3.6, there are only two FALs that result from well-paintings of this nerve. These are P_4 and C_2 .

Case 2: If F_N has been subdivided, then by Theorem 3.7, it must contain a buckle. Then, by Theorem 3.4, any FAL of this form is the belt-sum of two others, and therefore is not prime.

So the only two belt-sum prime cuboctahedral FALs are the two aforementioned FALs. \square

The consequence of this theorem is that every 1st family member is some belt-sum of these two links. In fact, we can make an even stronger claim in Theorem 3.10:

Lemma 3.9. The 1st family is closed under belt-summing.

Proof. Suppose by way of contradiction that there was some 1st family member F , with nerve F_N , that was formed by belt-summing some combination of links, at least one of which is not in the 1st family. We know by Theorem 2.6 that F_N must be formed by some number of central triangular subdivisions of the simple cuboctahedral nerve. By Theorem 3.7, each of these subdivisions forms a buckle, which is the thrice-punctured sphere which belt-summing decomposes along. Additionally, the only buckles in F_N occur at these subdivisions, since by construction there are no other non-trivial 3-cycles in F_N , once-painted or otherwise. Therefore, F will be belt-sum decomposed along each of the subdivisions, which all correspond to one additional cuboctahedron. Since belt-sum decomposition is unique (Theorem 3.5) this is the only way that F can be decomposed. So F cannot be the belt-sum of a collection of links that includes a non-cuboctahedral FAL. \square

Theorem 3.10. Every belt-sum composite 1st family member F can be uniquely belt-sum decomposed into a combination of P_4 's and C_2 's. Additionally, if F has c crossing circles, then F can be decomposed into x P_4 's and y C_2 's, where $x + y = \frac{c-1}{3}$.

Proof. Let F be a cuboctahedral FAL with c crossing circles. By Theorem 3.5, we know that every FAL can be uniquely decomposed into belt-sum prime FALs. Theorem 3.8 states that P_4 and the C_2 are the only two belt-sum prime cuboctahedral FALs. Finally, by Lemma 3.9, we know that F can only be the belt-sum of cuboctahedral FALs. Altogether, this means that F has a unique decomposition into P_4 's and C_2 's.

We know from Corollary 2.6.1 that if F has c crossing circles, then its complement is formed by gluing $n = \frac{2c-2}{3}$ cuboctahedra together ($\frac{c-1}{3}$ in the top half, P_+ , and $\frac{c-1}{3}$ in the bottom half, P_-). If there are x copies of P_4 and y copies of C_2 , then there are a total of $2x + 2y$ cuboctahedra glued together to form F . Then, since $2x + 2y = n$ and $n = \frac{2c-2}{3}$, simplifying yields $x + y = \frac{c-1}{3}$. \square

Finally, we may use a result from Adams [1] to address the nature of the volume of every cuboctahedral FAL complement.

Lemma 3.11 (Adams). If F_1 and F_2 are two FALs with volumes V_1, V_2 , then their belted sum F_{1+2} has volume $V_1 + V_2$.

Theorem 3.12. If a 1st family member F is formed by belt-summing prime family members together n times, then the volume of F is $(n + 1) \times 24.092184\dots$

Proof. Let F be a cuboctahedral FAL that decomposes into $n+1$ prime family members. Then it is the result of exactly n belt-sum operations. Each prime family member contains 2 cuboctahedra, so the complement of F contains $2n + 2$ cuboctahedra. By Lemma 3.11, volume is preserved under belt summing, so the volume of the belt-sum (the volume of F , that is) is the sum of the volumes of each cuboctahedra; from SnapPy, we found that the volume of 1 cuboctahedron is 12.0461..., and multiplying $(2n + 2) \times 12.0461$ yields the given value. \square

4 Using Gluing Maps and Length Spectra to Find A Common Geodesic in a Subset of the 1st Family

The results of the previous section mean that cuboctahedral FALs are a rather simple class of links, at least in terms of belt-summing, since every cuboctahedral FAL can be built up from just two simple ones. We use this nice property to examine geodesics in cuboctahedral FALs.

4.1 Calculating The Systoles

We began by utilizing SnapPy to find the length spectra of both P_4 and C_2 with no half-twists. While geodesics beyond the systoles may be of interest for other purposes, our goal was only to examine the systoles (the shortest geodesics in the respective links' complements) and see where they were located. Figure 16 shows every geodesic of length less than 4.

Conveniently, both links share the exact same number of systoles of the exact same length and rotation. However, SnapPy only shows that they exist. It was up to us to locate them in the link complement.

4.2 Locating the Systoles

To find the systoles, we began by constructing the fundamental regions of both links. While these links conveniently possess the same exact shape, the labelling of the regions differs between the two, as certain shaded regions are paired different according to how the two links were decomposed. As a result, the gluing maps are different. Figure 17 shows how the two FALs were labelled. In both cases, we chose to send the point of tangency between A and A' to infinity, making Z the face along which the upper and lower halves of the link complements were glued together.

P_4			C_2		
Multiplicity	Length	Rotation	Multiplicity	Length	Rotation
8	2.5533737...	$-2.0534164...i$	8	2.5533737...	$-2.0534164...i$
8	2.5533737...	$2.0534164...i$	8	2.5533737...	$2.0534164...i$
29	3.5254943...	0	25	3.5254943...	$-3.3892015...i$
40	3.6261872...	$-2.4946975...i$	8	3.5254943...	$3.1415926...i$
40	3.6261872...	$2.4946975...i$	32	3.6261872...	$-2.4946975...i$
24	3.7556317...	$-0.9176411...i$	32	3.6261872...	$2.4946975...i$
24	3.7556317...	$0.9176411...i$	24	3.7556317...	$-0.9176411...i$
			24	3.7556317...	$0.9176411...i$
			12	3.8860507...	$-1.9490701...i$
			12	3.8860507...	$1.9490701...i$

Figure 16: Length Spectra for the Two Links



Figure 17: How The Regions of Both FALs Were Labelled.

The next step was to calculate the gluing maps for both links. To do this, we found the Möbius transformations using Maple, then wrote them all in matrix form. Then, we normalized the matrices and calculated their traces. We then plugged these traces into the hyperbolic length formula, $l = 2 \operatorname{arccosh}(\frac{\pm \operatorname{trace}}{2})$. Unsurprisingly, the lengths of almost every curve was 0, as they could be pushed arbitrarily close to a cusp, often around either crossing circles or planar components. The exceptions were the maps φ_X in both links and their inverses. But these had lengths longer than the systoles (length ≈ 3.52549), so they were not what we were looking for. The full gluing maps, including images of the curves they represent, are shown in Figures 18 and 19.

Map	Picture	Map	Picture
$\varphi_A = A \rightarrow A'$ $\varphi_A = \begin{bmatrix} 1 & 4\sqrt{2} \\ 0 & 1 \end{bmatrix}$		$\varphi_A^{-1} = A' \rightarrow A$ $\varphi_A^{-1} = \begin{bmatrix} 1 & -4\sqrt{2} \\ 0 & 1 \end{bmatrix}$	
$\varphi_{B_+} = B_+ \rightarrow B'_+$ $\varphi_{B_+} = \begin{bmatrix} 1 + 2\sqrt{2}i & 8\sqrt{2} \\ \frac{\sqrt{2}}{2} & 1 - 2\sqrt{2}i \end{bmatrix}$		$\varphi_{B_+}^{-1} = B'_+ \rightarrow B_+$ $\varphi_{B_+}^{-1} = \begin{bmatrix} 1 - 2\sqrt{2}i & -8\sqrt{2} \\ -\frac{\sqrt{2}}{2} & 1 + 2\sqrt{2}i \end{bmatrix}$	
$\varphi_{B_-} = B_- \rightarrow B'_-$ $\varphi_{B_-} = \begin{bmatrix} 1 - 2\sqrt{2}i & 8\sqrt{2} \\ \frac{\sqrt{2}}{2} & 1 + 2\sqrt{2}i \end{bmatrix}$		$\varphi_{B_-}^{-1} = B'_- \rightarrow B_-$ $\varphi_{B_-}^{-1} = \begin{bmatrix} 1 + 2\sqrt{2}i & -8\sqrt{2} \\ -\frac{\sqrt{2}}{2} & 1 - 2\sqrt{2}i \end{bmatrix}$	
$\varphi_{C_+} = C_+ \rightarrow C'_+$ $\varphi_{C_+} = \begin{bmatrix} 1 + \frac{\sqrt{2}}{2}i & -2i \\ \frac{1}{4}i & 1 - \frac{\sqrt{2}}{2}i \end{bmatrix}$		$\varphi_{C_+}^{-1} = C'_+ \rightarrow C_+$ $\varphi_{C_+}^{-1} = \begin{bmatrix} 1 - \frac{\sqrt{2}}{2}i & 2i \\ -\frac{1}{4}i & 1 + \frac{\sqrt{2}}{2}i \end{bmatrix}$	
$\varphi_{C_-} = C_- \rightarrow C'_-$ $\varphi_{C_-} = \begin{bmatrix} 1 - \frac{\sqrt{2}}{2}i & 2i \\ -\frac{1}{4}i & 1 + \frac{\sqrt{2}}{2}i \end{bmatrix}$		$\varphi_{C_-}^{-1} = C'_- \rightarrow C_-$ $\varphi_{C_-}^{-1} = \begin{bmatrix} 1 + \frac{\sqrt{2}}{2}i & -2i \\ \frac{1}{4}i & 1 - \frac{\sqrt{2}}{2}i \end{bmatrix}$	
$\varphi_D = D \rightarrow D'$ $\varphi_D = \begin{bmatrix} 1 & 0 \\ \frac{\sqrt{2}}{2} & 1 \end{bmatrix}$		$\varphi_D^{-1} = D' \rightarrow D$ $\varphi_D^{-1} = \begin{bmatrix} 1 & 0 \\ -\frac{\sqrt{2}}{2} & 1 \end{bmatrix}$	
$\varphi_U = U_+ \rightarrow U_-$ $\varphi_U = \begin{bmatrix} 1 - \sqrt{2}i & -4i \\ \frac{1}{2}i & 1 + \sqrt{2}i \end{bmatrix}$		$\varphi_U^{-1} = U_- \rightarrow U_+$ $\varphi_U^{-1} = \begin{bmatrix} 1 + \sqrt{2}i & 4i \\ -\frac{1}{2}i & 1 - \sqrt{2}i \end{bmatrix}$	
$\varphi_V = V_+ \rightarrow V_-$ $\varphi_V = \begin{bmatrix} 1 + \sqrt{2}i & -4i \\ \frac{1}{2}i & 1 - \sqrt{2}i \end{bmatrix}$		$\varphi_V^{-1} = V_- \rightarrow V_+$ $\varphi_V^{-1} = \begin{bmatrix} 1 - \sqrt{2}i & 4i \\ -\frac{1}{2}i & 1 + \sqrt{2}i \end{bmatrix}$	
$\varphi_W = W_+ \rightarrow W_-$ $\varphi_W = \begin{bmatrix} 1 & 0 \\ i & 1 \end{bmatrix}$		$\varphi_W^{-1} = W_- \rightarrow W_+$ $\varphi_W^{-1} = \begin{bmatrix} 1 & 0 \\ -i & 1 \end{bmatrix}$	
$\varphi_X = X_+ \rightarrow X_-$ $\varphi_X = \begin{bmatrix} 3 & -8i \\ i & 3 \end{bmatrix}$		$\varphi_X^{-1} = X_- \rightarrow X_+$ $\varphi_X^{-1} = \begin{bmatrix} 3 & 8i \\ -i & 3 \end{bmatrix}$	
$\varphi_Y = Y_+ \rightarrow Y_-$ $\varphi_Y = \begin{bmatrix} 1 & -8i \\ 0 & 1 \end{bmatrix}$		$\varphi_Y^{-1} = Y_- \rightarrow Y_+$ $\varphi_Y^{-1} = \begin{bmatrix} 1 & 8i \\ 0 & 1 \end{bmatrix}$	

Figure 18: Table of Gluing Maps for P4

Map	Picture	Map	Picture
$\varphi_A = A \rightarrow A'$ $\varphi_A = \begin{bmatrix} 1 & -4\sqrt{2} \\ 0 & 1 \end{bmatrix}$		$\varphi'_A = A' \rightarrow A$ $\varphi_A^{-1} = \begin{bmatrix} 1 & 4\sqrt{2} \\ 0 & 1 \end{bmatrix}$	
$\varphi_{B_+} = B_+ \rightarrow B'_+$ $\varphi_{B_+} = \begin{bmatrix} 1 + 2\sqrt{2}i & -4\sqrt{2} \\ \sqrt{2} & -1 + 2\sqrt{2}i \end{bmatrix}$		$\varphi_{B_+}^{-1} = B'_+ \rightarrow B_+$ $\varphi_{B_+}^{-1} = \begin{bmatrix} -1 + 2\sqrt{2}i & 4\sqrt{2} \\ -\sqrt{2} & 1 + 2\sqrt{2}i \end{bmatrix}$	
$\varphi_{B_-} = B_- \rightarrow B'_-$ $\varphi_{B_-} = \begin{bmatrix} -1 + 2\sqrt{2}i & -4\sqrt{2} \\ \sqrt{2} & 1 + 2\sqrt{2}i \end{bmatrix}$		$\varphi_{B_-}^{-1} = B'_- \rightarrow B_-$ $\varphi_{B_-}^{-1} = \begin{bmatrix} 1 + 2\sqrt{2}i & 4\sqrt{2} \\ -\sqrt{2} & -1 + 2\sqrt{2}i \end{bmatrix}$	
$\varphi_{C_+} = C_+ \rightarrow C'_+$ $\varphi_{C_+} = \begin{bmatrix} \sqrt{2}i & 2\sqrt{2} \\ \frac{\sqrt{2}}{4} - i & -2 - \sqrt{2}i \end{bmatrix}$		$\varphi_{C_+}^{-1} = C'_+ \rightarrow C_+$ $\varphi_{C_+}^{-1} = \begin{bmatrix} -2 - \sqrt{2}i & -2\sqrt{2} \\ -\frac{\sqrt{2}}{4} + i & \sqrt{2}i \end{bmatrix}$	
$\varphi_{C_-} = C_- \rightarrow C'_-$ $\varphi_{C_-} = \begin{bmatrix} \sqrt{2}i & -2\sqrt{2} \\ -\frac{\sqrt{2}}{4} - i & 2 - \sqrt{2}i \end{bmatrix}$		$\varphi_{C_-}^{-1} = C'_- \rightarrow C_-$ $\varphi_{C_-}^{-1} = \begin{bmatrix} 2 - \sqrt{2}i & 2\sqrt{2} \\ \frac{\sqrt{2}}{4} + i & \sqrt{2}i \end{bmatrix}$	
$\varphi_{D_+} = D_+ \rightarrow D'_+$ $\varphi_{D_+} = \begin{bmatrix} \sqrt{2}i & 2\sqrt{2} \\ \frac{\sqrt{2}}{4} + i & 2 - \sqrt{2}i \end{bmatrix}$		$\varphi_{D_+}^{-1} = D'_+ \rightarrow D_+$ $\varphi_{D_+}^{-1} = \begin{bmatrix} 2 - \sqrt{2}i & -2\sqrt{2} \\ -\frac{\sqrt{2}}{4} - i & \sqrt{2}i \end{bmatrix}$	
$\varphi_{D_-} = D_- \rightarrow D'_-$ $\varphi_{D_-} = \begin{bmatrix} \sqrt{2}i & -2\sqrt{2} \\ -\frac{\sqrt{2}}{4} - i & -2 - \sqrt{2}i \end{bmatrix}$		$\varphi_{D_-}^{-1} = D'_- \rightarrow D_-$ $\varphi_{D_-}^{-1} = \begin{bmatrix} -2 - \sqrt{2}i & 2\sqrt{2} \\ \frac{\sqrt{2}}{4} + i & \sqrt{2}i \end{bmatrix}$	
$\varphi_U = U_+ \rightarrow U_-$ $\varphi_U = \begin{bmatrix} 1 - \sqrt{2}i & -4i \\ \frac{1}{2}i & 1 + \sqrt{2}i \end{bmatrix}$		$\varphi_U^{-1} = U_- \rightarrow U_+$ $\varphi_U^{-1} = \begin{bmatrix} 1 + \sqrt{2}i & 4i \\ -\frac{1}{2}i & 1 - \sqrt{2}i \end{bmatrix}$	
$\varphi_V = V_+ \rightarrow V_-$ $\varphi_V = \begin{bmatrix} 1 + \sqrt{2}i & -4i \\ \frac{1}{2}i & 1 - \sqrt{2}i \end{bmatrix}$		$\varphi_V^{-1} = V_- \rightarrow V_+$ $\varphi_V^{-1} = \begin{bmatrix} 1 - \sqrt{2}i & 4i \\ -\frac{1}{2}i & 1 + \sqrt{2}i \end{bmatrix}$	
$\varphi_W = W_+ \rightarrow W_-$ $\varphi_W = \begin{bmatrix} 1 & 0 \\ i & 1 \end{bmatrix}$		$\varphi_W^{-1} = W_- \rightarrow W_+$ $\varphi_W^{-1} = \begin{bmatrix} 1 & 0 \\ -i & 1 \end{bmatrix}$	
$\varphi_X = X_+ \rightarrow X_-$ $\varphi_X = \begin{bmatrix} 3 & -8i \\ i & 3 \end{bmatrix}$		$\varphi_X^{-1} = X_- \rightarrow X_+$ $\varphi_X^{-1} = \begin{bmatrix} 3 & 8i \\ -i & 3 \end{bmatrix}$	
$\varphi_Y = Y_+ \rightarrow Y_-$ $\varphi_Y = \begin{bmatrix} 1 & -8i \\ 0 & 1 \end{bmatrix}$		$\varphi_Y^{-1} = Y_- \rightarrow Y_+$ $\varphi_Y^{-1} = \begin{bmatrix} 1 & 8i \\ 0 & 1 \end{bmatrix}$	

Figure 19: Table of Gluing Maps for C_2

Since none of these maps were systoles, we had to multiply matrices to find more complicated curves in the manifold, with the intention of finding a matrix whose trace was $2 \pm 2\sqrt{2}i$. This trace corresponded to the length of the systoles that we were searching for. The table in Figures 20 and 21 lists all the systoles as products of gluing maps for both links.

Systoles With Positive Rotation	Systoles With Negative Rotation
$\varphi_{A_+} \varphi_U$	$\varphi_{A_+}^{-1} \varphi_U$
$\varphi_{A_+} \varphi_V$	$\varphi_{A_+}^{-1} \varphi_V$
$\varphi_{A_-} \varphi_U$	$\varphi_{A_-}^{-1} \varphi_U$
$\varphi_{A_-} \varphi_V$	$\varphi_{A_-}^{-1} \varphi_V$
$\varphi_{D_+}^{-1} \varphi_U$	$\varphi_{D_+} \varphi_U$
$\varphi_{D_+}^{-1} \varphi_V$	$\varphi_{D_+} \varphi_V$
$\varphi_{D_-}^{-1} \varphi_U$	$\varphi_{D_-} \varphi_U$
$\varphi_{D_-}^{-1} \varphi_V$	$\varphi_{D_-} \varphi_V$

Figure 20: Every Systole for P_4 in Terms of Gluing Maps

Systoles With Positive Rotation	Systoles With Negative Rotation
$\varphi_{A_+}^{-1} \varphi_U$	$\varphi_{A_+} \varphi_U$
$\varphi_{A_+}^{-1} \varphi_V$	$\varphi_{A_+} \varphi_V$
$\varphi_{A_-}^{-1} \varphi_U$	$\varphi_{A_-} \varphi_U$
$\varphi_{A_-}^{-1} \varphi_V$	$\varphi_{A_-} \varphi_V$
$\varphi_{C_+} \varphi_U$	$\varphi_{C_+} \varphi_W$
$\varphi_{C_-} \varphi_U$	$\varphi_{C_-} \varphi_W$
$\varphi_{D_+} \varphi_W$	$\varphi_{D_+} \varphi_V$
$\varphi_{D_-} \varphi_W$	$\varphi_{D_-} \varphi_V$

Figure 21: Every Systole for C_2 in Terms of Gluing Maps

4.3 Every Thrice-Punctured Sphere's Complement Contains a Systole

Now that we have the locations of every systole in both links, the next step is to locate every thrice-punctured sphere.

Lemma 4.1 (Morgan et. al.). There are only three types of thrice-punctured spheres in the complement of an FAL, defined as follows:

- Standard thrice punctured spheres, which are formed by crossing circles. These correspond to painted edges in a nerve.
- Buckle thrice-punctured spheres, which correspond to buckles in the nerve (once-painted non-trivial 3-cycles)
- K_4 thrice-punctured spheres, which correspond to K_4 subgraphs in the nerve (K_4 being the complete graph on 4 vertices)

Lemma 4.2. P_4 and C_2 contain only standard thrice-punctured spheres.

Proof. Examining the nerves of P_4 and C_2 , it is clear that neither nerve contains a K_4 subgraph, since there are no non-trivial 3-cycles. We also know that these are belt-sum prime nerves, and therefore they contain no buckles. So the only thrice-punctured spheres in these two links are the 4 crossing circles in each. \square

Lemma 4.3. All 1st family members that are not P_4 and C_2 contain only standard thrice-punctured spheres and buckle thrice-punctured spheres.

Proof. Let F be a 1st family member that is not P_4 or C_2 . Then it must be belt-sum composite by Theorem 3.8. Then it must contain a buckle by Theorem 3.4, so it will contain buckle thrice-punctured spheres. Additionally, we know from Corollary 2.6.1 that it will contain $\frac{3}{2}n + 1$ crossing circles, where n is the number of cuboctahedra forming F . It remains to show that there are no K_4 thrice-punctured spheres in F . But in order for F_N to contain a K_4 subgraph, we must have subdivided some trivial 3-cycle at some point in the series of subdivisions performed to obtain F_N in a different manner, namely, adding one vertex inside the triangle and connecting it to each other vertex. But by Theorem 2.6 this cannot be the case, so no K_4 punctured spheres will exist in any 1st family member. \square

Lemma 4.4. The complement of any thrice-punctured sphere in P_4 will contain a geodesic of length 2.5533....

Proof. By Lemma 4.3, there are 4 possible thrice-punctured spheres to choose from in P_4 ; these are the 4 crossing circles. If we choose to belt-sum by cutting along circles B or C (see Figure 17), then every systole will be in the complement.

If we cut along crossing circle A , then there are 8 systoles in its complement, these being the curves formed by φ_U , φ_V , and the inverses and upper and lower counterparts for φ_D . Similarly, if we cut along crossing circle D , then the other 8 systoles (formed by φ_A , φ_U , and φ_V) are in the complement. So the complement of every thrice-punctured sphere contained multiple geodesics of length 2.5533.... \square

Lemma 4.5. The complement of any thrice-punctured sphere in C_2 will contain a geodesic of length 2.5533....

Proof. Similar to the proof for the previous lemma, there are 4 crossing circles that we can choose to cut along. If we choose to cut along B , then every systole is in the complement of that thrice-punctured sphere.

If we cut along A , then the 8 systoles containing either φ_C or φ_D will be in the complement.

If we cut along C , then every systole containing φ_A and φ_D will be in the complement. Similarly, cutting alone D means systoles containing φ_A and φ_C are in the complement.

So the complement of every thrice-punctured sphere in C_2 contains a geodesic of length 2.5533.... \square

Lemma 4.6. The complement of any buckle thrice punctured sphere will contain a geodesic of length 2.5533....

Proof. Suppose F is a 1st family member containing buckle thrice-punctured spheres. Then it has been formed by belt-summing some number of times; consider the most recent of these. In this case, we take some other 1st family member L and either belt-sum P_4 or C_2 to it by cutting along a thrice-punctured sphere in each of the links and attaching them together in order to form F . By Lemmas 4.4 and 4.5, both P_4 and C_2 have geodesics of length 2.5533... in the complements of any standard thrice-punctured sphere we choose to belt-sum along, the resulting F will contain a geodesic of this length as well. \square

Theorem 4.7. The complement of any thrice-punctured sphere in a flat 1st family member will contain a geodesic of length 2.5533....

Proof. Suppose F is a flat first family member with painted nerve F_N . If F_N has not been subdivided, it is either P_4 or C_2 . Then by Lemmas 4.4 and 4.5, F contains a geodesic of length 2.5533....

Now suppose F has been subdivided at least once. Then by Lemma 4.3, the only thrice-punctured spheres in F are standard and buckle thrice-punctured spheres. We know that the complement of every standard thrice-punctured sphere will contain a geodesic of length 2.5533... by Lemmas 4.4 and 4.5. Additionally, the complements of the buckle thrice-punctured spheres must also contain these geodesics by Lemma 4.6. \square

Corollary 4.7.1. If a link does not contain a geodesic of length 2.5533... in its length spectrum, then it is not a flat 1st family member.

Proof. This is a direct consequence of the previous theorem. Since the complement of every thrice-punctured sphere in a cuboctahedral FAL contains a geodesic of length 2.5533..., then there will be a geodesic of this length in the complement of every cuboctahedral FAL. \square

5 Further Questions

Everything described above is the extent of our findings. There are however, questions closely related to these topics that are still unanswered, which we list and explain here.

- Does the belt-sum operation create shorter geodesics?

If the above is true, then the result in Corollary 4.7.1 is as strong a claim as we can make regarding the length spectra of cuboctahedral FALs. However, if the answer is false, and belt-summing preserves systolic length, then the following stronger claim will be true:

Conjecture 1. The systolic length of every flat 1st family member is 2.5533....

- How will the presence of half-twists affect systole length in the two belt-sum prime links?
- Are there other classes of FALs for which similar results can be found?

While we restricted ourselves to cuboctahedral FALs since together with octahedral FALs they represent all arithmetic FALs as recently proven by Worden and Hoffman [6], there are other polyhedra that tessellate hyperbolic space in a similar manner including regular ideal tetrahedra. . Are there FALs whose complements are formed by gluing of these polyhedra instead, and can a similar endeavor be undertaken on those classes as we have done here with cuboctahedral FALs?

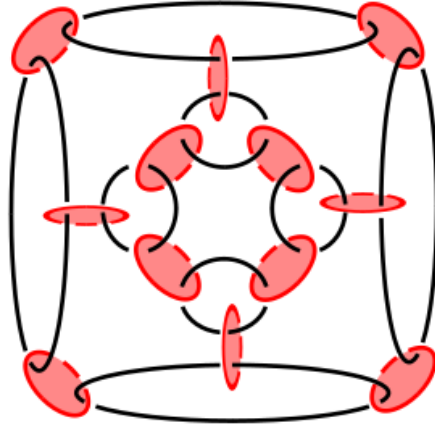


Figure 22: Cuboctahedral FAL not in the 1st family.

- Our work is limited to just one family of cuboctahedral FALs. We know for a fact that there exists at least one more family; the link shown above is one of its members. This link decomposes into cuboctahedra through a different process than the one we described (one that does not respect the preferred horoball packing), and its nerve does not follow our characterization.
 - Is this the only other family, or are there more?
 - Can we perform a similar analysis on this family (and others)?
 - What happens when we belt-sum members of two families together?
 - The list of questions goes on.

Acknowledgements

The sincerest of thanks goes to my advisor, Rolland Trapp. I would also like to thank the NSF and CSUSB for helping support this program, Dr. Corey Dunn for his role in this REU, and all my peers who I worked alongside during this research. This research was funded under NSF grant number DMS-2050894.

6 References

References

- [1] Colin C. Adams. “Thrice-Punctured Spheres in Hyperbolic 3-Manifolds” (1985), p. 654.
- [2] Colin Machlachlan and Alan W. Reid. “The Arithmetic of Hyperbolic 3-Manifolds”. Graduate Texts in Mathematics. Springer, 2003. Chap. 12.1.
- [3] Jeffrey Meyer, Christian Millichap, and Rolland Trapp. “Arithmeticity and Hidden Symmetries of Fully Augmented Pretzel Link Complements” (2018).
- [4] Porter Morgan et al. “Belted-Sum Decompositions of Fully Augmented Links” (Manuscript in pre-print).
- [5] Jessica S. Purcell. “An Introduction to Fully Augmented Links” (2011).
- [6] William Worden and Neil Hoffman (private communication).

Emerson Worrell
Mathematics Department
Colorado College
Colorado Springs, CO 80946
Email: *e.worrell@coloradocollege.edu*